

Dephasing of Transverse Spin Current in Ferrimagnetic Alloys

Youngmin Lim¹, Behrouz Khodadadi¹, Jie-Fang Li², Dwight Viehland², Aurelien Manchon^{3,4},

Satoru Emori^{1,*}

1. Department of Physics, Virginia Tech, Blacksburg, VA 24061, USA

2. Department of Materials Science and Engineering, Virginia Tech, Blacksburg, VA 24061,
USA

3. Physical Science and Engineering Division (PSE), King Abdullah University of Science and
Technology (KAUST), Thuwal 23955-6900, Saudi Arabia

4. Aix-Marseille Univ, CNRS, CINaM, Marseille, France

* email: semori@vt.edu

It has been predicted that transverse spin current can propagate coherently (without dephasing) over a long distance in antiferromagnetically ordered metals. Here, we determine the dephasing length of transverse spin current in ferrimagnetic CoGd alloys by spin pumping measurements. A modified drift-diffusion model, which accounts for spin-current transmission through the ferrimagnet, reveals a dephasing length in nearly compensated CoGd that is about 4-5 times longer than that in ferromagnetic metals. Our results confirm partial mitigation of spin dephasing in antiferromagnetically ordered metals, analogous to spin echo rephasing for nuclear and qubit spin systems.

A spin current is said to be coherent when the spin polarization of its carriers, such as electrons, is locked in a uniform orientation or precessional phase. How far a spin current propagates before decohering underpins various phenomena in solids [1,2]. Spin decoherence can generally arise from *spin-flip scattering*, where the carrier spin polarization is randomized via momentum scattering [3,4]. Moreover, in magnetic materials, electronic spin current polarized transverse to the magnetization can decohere by *dephasing*, where the total carrier spin polarization vanishes due to averaging [5–9]. As illustrated in Fig. 1(a), electronic spins enter the ferromagnetic metal (FM) with the same phase but precess about the exchange field at different rates. The different precession rates arise due to these electronic spins having a wide distribution of incident wavevectors (momenta) spanned by the Fermi surface of the FM, such that they spend different amounts of time in the exchange field¹. Within a few atomic monolayers in the FM, the transverse spin polarization averages to zero, i.e., the spin current dephases [5–9]. In typical FMs, the dephasing length λ_{dp} is only ≈ 1 nm [5–7,10] whereas the transverse spin-flip (diffusion) length λ_{sf} may be considerably longer (e.g., ≈ 10 nm) [3,4], such that dephasing dominates the decoherence of transverse spin current.

Transverse spin currents in antiferromagnetically ordered metals have been predicted to exhibit longer λ_{dp} [11–14]. This prediction may apply not only to intrinsic antiferromagnetic metals (AFMs) but also compensated ferrimagnetic metals (FIMs) that consist of antiferromagnetically coupled transition-metal (TM) and rare-earth-metal (RE) magnetic sublattices [15]. In the ideal case as illustrated in Fig. 1(b), the spin current interacts with the staggered antiferromagnetic exchange field whose direction alternates at the atomic length scale. The propagating spins precess in alternating directions as they move from one magnetic sublattice to the next, such that spin dephasing is suppressed over multiple monolayers. This

¹ An insulating tunnel barrier is known to filter the incident wavevectors to a narrow distribution [81], which can extend λ_{dp} .

cancellation of dephasing in AFM/FIMs is analogous to spin rephasing by π -pulses (Hahn spin echo method) in nuclear magnetic resonance [16], which has recently inspired several approaches of mitigating decoherence of qubit spin systems [17–19].

The above idealized picture for extended coherence in antiferromagnetically ordered metals (Fig. 1(b)) assumes a spin current without any scattering and simple layer-by-layer alternating collinear magnetic order. Finite scattering, spin-orbit coupling, and complex magnetization states in real materials may disrupt transverse spin coherence [20–22]. A shorter overall coherence length² results from reduced λ_{sf} due to increased spin-flip rates, or reduced λ_{dp} due to momentum scattering and non-collinear magnetic order that prevents perfect cancellation of dephasing [20,21]. Most experiments on AFMs (e.g., polycrystalline IrMn) indeed show short coherence lengths of typically ≈ 1 nm [7,23–26]. Nevertheless, a recent experimental study utilizing a spin galvanic detection method [27,28] has reported a long coherence length in excess of 10 nm, attributed to the suppression of dephasing, at room temperature in FIMs of CoTb [15]. The report in Ref. [15] is quite surprising considering the strong spin-orbit coupling of CoTb, primarily from RE Tb with a large orbital angular momentum, which can result in increased spin-flip scattering [29–31] and noncollinear sperimagnetic order [32–34]. TM and RE elements also tend to form amorphous alloys [32–35], whose structural disorder may result in further scattering and deviation from layer-by-layer antiferromagnetic order. It therefore remains a critical issue to confirm whether the cancellation of dephasing (as depicted in Fig. 1(b)) actually extends transverse spin coherence in antiferromagnetically ordered metals, particularly structurally disordered FIMs.

Here, we present a quantitative test for the suppressed dephasing of transverse spin current in ferrimagnetic alloys. Our test consists of ferromagnetic resonance (FMR) spin

² The transverse coherence length λ_c can be defined as $1/\lambda_c = \text{Re} \left[\sqrt{(1/\lambda_{sf}^2) - (i/\lambda_{dp}^2)} \right]$ [10,82].

pumping measurements [7,24] on a series of amorphous FIM CoGd spin sinks, which exhibit significantly weaker spin-orbit coupling than CoTb due to the nominally zero orbital angular momentum of RE Gd. Our experimental results combined with a modified drift-diffusion model [9,10,36,37] reveal that spin dephasing is indeed partially cancelled in nearly compensated CoGd, with λ_{dp} extended by a factor of 4-5 compared to that for FMs. This finding confirms that, even in the presence of substantial structural disorder, the antiferromagnetic order in FIMs can mitigate the decoherence of transverse spin current. Overall, our work takes a crucial step towards understanding the fundamental interplay between spin current and antiferromagnetic order.

The samples investigated here are $\text{Ni}_{80}\text{Fe}_{20}(7)/\text{Cu}(4)/\text{Co}_{100-x}\text{Gd}_x(d)$ trilayers (unit: nm) with $x = 0, 20, 22, 23, 25, 28$, and 30 ; details of film growth and stack structure are in the Supplemental Material [38]. A coherent spin current generated by FMR [39,40] in NiFe propagates through the diamagnetic Cu spacer and decoheres in the $\text{Co}_{100-x}\text{Gd}_x$ spin sink, yielding nonlocal Gilbert damping [7,24]. The Cu spacer layer suppresses static exchange coupling between the NiFe and CoGd layers [38]. The diamagnetic Cu spacer also accommodates spin transport mediated solely by conduction electrons, such that direct interlayer magnon coupling [14,41–43] does not play a role here. Vibrating sample magnetometry [38] reveals the magnetic compensation composition for $\text{Co}_{100-x}\text{Gd}_x$ thin films to be $x \approx 22-26$, consistent with prior reports [44,45]. The angular momentum compensation composition is only ≈ 1 Gd at. % below the magnetic compensation composition, since the g -factors of Co and Gd are similar ($g_{\text{Co}} \approx 2.15$, $g_{\text{Gd}} = 2.0$) [46]. CoGd layers in our stack structures do not show perpendicular magnetic anisotropy [15,47–56], i.e., CoGd films here are in-plane magnetized [44,45,57,58].

In our FMR spin pumping measurements, the half-width-at-half-maximum linewidth ΔH of the NiFe layer is measured via field-sweep measurements at microwave frequencies $f = 2-20$ GHz [38]. The FMR response of the NiFe layer is readily deconvoluted from that of pure Co ($x =$

0), and CoGd did not yield FMR signals above our instrumental background [38]. Thus, as shown in Fig. 2, the Gilbert damping parameter α for the NiFe layer is quantified from the f dependence of ΔH through the standard linear fit, $\mu_0 \Delta H = \mu_0 \Delta H_0 + \frac{h}{g \mu_B} \alpha f$, where $g \approx 2.1$ is the Landé g -factor of $\text{Ni}_{80}\text{Fe}_{20}$, μ_0 is the permeability of free space, h is Planck's constant, μ_B is the Bohr magneton, $\mu_0 \Delta H_0$ (< 0.2 mT) is the zero-frequency linewidth attributed to magnetic inhomogeneity [59]. For NiFe without a spin sink, we obtain $\alpha_{\text{no-sink}} \approx 0.0067$, similar to typically reported values for $\text{Ni}_{80}\text{Fe}_{20}$ [60,61].

A finite thickness d of spin sink results in a damping parameter $\alpha_{\text{w/sink}}$ that is greater than $\alpha_{\text{no-sink}}$. For example, the damping increases significantly with just $d = 1$ nm of Co (Fig. 2(a)), suggesting substantial spin absorption by the spin sink. By contrast, a stack structure that includes an insulating layer of Ti-oxide before the spin sink does not show the enhanced damping (Fig. 2(a)). This observation is consistent with the Ti-oxide layer blocking the spin current [62,63] between the spin source and spin sink layers. Thus, the enhanced damping $\Delta\alpha = \alpha_{\text{w/sink}} - \alpha_{\text{no-sink}}$ is nonlocal in origin, i.e., due to the spin current propagating through the Cu spacer and decohering in the magnetic spin sink [7,10,24,36,39,40]. The decoherence of transverse spin current in the spin sink is then directly related to $\Delta\alpha$. This method is more straightforward to interpret than the method in Ref. [15] based on a dc spin galvanic signal, which could include significant parasitic contributions unrelated to spin transport [64–68].

In contrast to the large $\Delta\alpha$ with an ultrathin FM Co spin sink, the damping enhancement with d is more gradual for FIM CoGd sinks. Figure 2(b) shows exemplary linewidth versus frequency results where the spin sink is $\text{Co}_{75}\text{Gd}_{25}$, a composition close to magnetic compensation. A damping enhancement similar in magnitude to that of the 1-nm-thick FM Co spin sink is reached only when the $\text{Co}_{75}\text{Gd}_{25}$ thickness is several nm. This suggests that transverse spin-current decoherence takes place over a length scale $\gg 1$ nm.

As summarized in Fig. 3, the damping enhancement (i.e., transverse spin decoherence) for each spin sink composition saturates above a sufficiently large d . This apparent saturation thickness –related to how far the transverse spin current remains coherent [7,10] – changes markedly with the spin sink composition. With FM Co as the spin sink, the saturation of $\Delta\alpha$ occurs at $d \approx 1$ nm, in agreement with λ_{dp} reported before for FMs [7,10]. By contrast, $\Delta\alpha$ saturates at $d \gg 1$ nm for FIM CoGd sinks. This observation is qualitatively consistent with the partial cancellation of dephasing by compensated magnetic order in FIM CoGd, enabling transverse spin coherence deeper into the spin sink.

At this point, what is needed is a model to fit our experimental results for the series of CoGd spin sinks (symbols in Fig. 3, left column) and quantify λ_{dp} in a physically consistent way. The conventional drift-diffusion model captures spin-flip scattering in nonmagnetic metals [39,69,70], but not spin dephasing that is expected to be significant in magnetic metals. This conventional model also predicts a monotonic increase of $\Delta\alpha$ with spin sink thickness [39,69,70], whereas we observe non-monotonic behavior where $\Delta\alpha$ seems to overshoot before approaching saturation. For spin pumping studies with magnetic spin sinks, typical models assume complete spin dephasing within a length scale much shorter than the spin sink thickness (i.e., $\lambda_{dp} = 0$) [40,70,71]. Others fit a linear increase of $\Delta\alpha$ with d up to apparent saturation, deriving $\lambda_{dp} = 1.2 \pm 0.1$ nm for FMs [7,24,72]. However, it is questionable that this linear cut-off model applies in a physically meaningful way to our experimental results (Fig. 3), in which the increase of $\Delta\alpha$ to saturation is not generally linear.

We therefore apply an alternative model that captures the dephasing (i.e., precession and decay) of transmitted transverse spin current in the magnetic spin sinks by invoking the *transmitted spin-mixing conductance* $g_t^{\uparrow\downarrow}$ [5,9,10,36,37,73,74]. Although $g_t^{\uparrow\downarrow}$ is analogous to the conventional (reflected) spin-mixing conductance $g_r^{\uparrow\downarrow}$ at the spin sink interface, $g_t^{\uparrow\downarrow}$ is a function of the magnetic spin sink thickness d that vanishes in the limit of $d \gg \lambda_{dp}$ [5,9,73,74].

Furthermore, whereas $g_r^{\uparrow\downarrow}$ is essentially a positive real quantity, $g_t^{\uparrow\downarrow}(d)$ is a complex value where the real and imaginary parts are comparable in magnitude [74]; $\text{Re}[g_t^{\uparrow\downarrow}(d)]$ and $\text{Im}[g_t^{\uparrow\downarrow}(d)]$ are related to the transverse spin components, respectively, within and normal to the plane defined by the magnetic order and the incident spin polarization (cf. Fig. 2(b) in Ref. [9]). We approximate $g_t^{\uparrow\downarrow}(d)$ with an oscillatory decay function [9],

$$g_t^{\uparrow\downarrow}(d) = g_{t,0}^{\uparrow\downarrow} \left(\frac{\lambda_{dp}}{\pi d} \sin \frac{\pi d}{\lambda_{dp}} \pm i \left[\left(\frac{\lambda_{dp}}{\pi d} \right)^2 \sin \frac{\pi d}{\lambda_{dp}} - \frac{\lambda_{dp}}{\pi d} \cos \frac{\pi d}{\lambda_{dp}} \right] \right) \exp \left(-\frac{d}{\lambda_{sf}} \right), \quad (1)$$

where $g_{t,0}^{\uparrow\downarrow}$ is a complex coefficient. The positive (negative) sign between the real and imaginary terms corresponds to the net spin precession direction about an effective exchange field along (opposing) the net magnetization; while the effective exchange field is along the net magnetization in most cases, we later discuss a case where the exchange field opposes the net magnetization. The exponential factor with λ_{sf} approximates incoherent scattering as an additional source of spin-current decoherence.

We incorporate Eq. (1) into the drift-diffusion model [10] that uses the boundary conditions applicable to our multilayer systems. While we refer the readers to Ref. [10] and the Supplemental Material [38] for details, we briefly list some key assumptions that constrain the number of free parameters to fit our experimental results. First, the spin-flip length is set at $\lambda_{sf} = 10$ nm, similar to reported spin diffusion lengths in FMs [4]. Second, the NiFe/Cu and Cu/Co interfaces are assumed to have the same $g_r^{\uparrow\downarrow}$, in line with the conventional understanding that $g_r^{\uparrow\downarrow}$ at a FM/normal-metal interface is primarily determined by the normal metal [7,75]. Lastly, $\text{Re}[g_{t,0}^{\uparrow\downarrow}]$ in Eq. (1) is set constant for $\text{Co}_{100-x}\text{Gd}_x$ with $x = 22-30$, where the magnitude of the net exchange splitting is small [38]. We are therefore left with only two free fit parameters: λ_{dp} and $\text{Im}[g_{t,0}^{\uparrow\downarrow}]$. The latter represents the amplitude of net transverse spin precession about the magnetic order.

The fit results using the modified drift-diffusion model are shown as solid curves in Fig. 3. These fit curves adequately reproduce the d dependence of $\Delta\alpha$ for all spin sink compositions. We also show in Fig. 3 the corresponding d dependence of $g_t^{\uparrow\downarrow}$, illustrating the net precession and decay of the transverse spin current in the magnetic spin sinks.

With the modeled results in Fig. 3, the overshoot in $\Delta\alpha$ versus d can now be attributed to the precession of the transverse spin current [9,37,73]. For a certain magnetic spin sink thickness, the polarization of the spin current leaving the sink is opposite to that of the spin current entering the spin sink; since the difference between the leaving and entering spin currents is related to the spin angular momentum transferred to the magnetic order, the spin transfer – manifesting as $\Delta\alpha$ here – can be enhanced [9,37,73] compared to when the spin current is completely dephased for $d \gg \lambda_{dp}$.

In Fig. 4(a), we summarize the composition dependence of λ_{dp} , derived from our model (vertical dashed lines in Fig. 3). Pure Co exhibits a short λ_{dp} of 1.3 ± 0.1 nm consistent with previous results on FM spin sinks [7]. By contrast, a significantly longer λ_{dp} of 5.3 ± 0.2 nm is obtained for the $\text{Co}_{75}\text{Gd}_{25}$ spin sink, whose composition is within the magnetic compensation window of $x \approx 22\text{--}26$ [38]. With further increase in Gd content, λ_{dp} decreases to 3.1 ± 1.1 nm for $\text{Co}_{70}\text{Gd}_{30}$. These results indicate that λ_{dp} has a non-monotonic dependence on the Gd concentration, with the peak approximately coinciding with magnetic compensation.

Our results are consistent with the theoretical prediction that antiferromagnetic order mitigates the decoherence of transverse spin current [11–15]. In a nearly compensated FIM CoGd spin sink, the alternating Co and Gd moments of approximately equal magnitude (as qualitatively illustrated by the alternating blue and green vertical arrows in Fig. 1(b)) partially cancel the dephasing of the propagating spins. Transverse spin current in compensated CoGd is therefore able to remain coherent over a longer distance than in FMs, although it does

decohere within a finite length scale due to the imperfect suppression of dephasing and the presence of incoherent scattering.

In addition to the enhanced λ_{dp} , a minimum in $\text{Im}[g_{t,0}^{\uparrow\downarrow}]$ is observed around the magnetic compensation composition (Fig. 4(b)). This finding corroborates the scenario where the nearly compensated magnetic sublattices reduces the net spin precession amplitude. Our results in Figs. 3 and 4 therefore consistently point to the suppression of spin-current dephasing enabled by antiferromagnetic order.

It is important to note that FIM TM-RE alloys in general are amorphous with no long-range structural order. Instead of the simple layer-by-layer alternating order illustrated in Fig. 1(b), the TM and RE atoms are expected to be arranged in a rather disordered fashion. Considering that disorder and electronic scattering tend to quench transverse spin coherence [15,20,21], it is remarkable that such amorphous FIMs permit extended λ_{dp} at all. We speculate the observed enhancement of transverse spin coherence is enabled by short-range ordering of Co and Gd atoms, e.g., finite TM-TM and RE-RE pair correlations in the film plane (and TM-RE pair correlation out of the film plane) as suggested by prior reports [15,76].

More generally, it might be expected that transverse spin current interacts more strongly with the Co magnetization (from the spin-split itinerant $3d$ bands near the Fermi level) [48,77] than the Gd magnetization (primarily from the localized $4f$ levels ≈ 7 -8 eV below the Fermi level [78,79]) – analogous to magnetotransport phenomena dominated by itinerant $3d$ band magnetism in TM-RE FIMs [45,80]. We observe evidence of this in the modeling result for $\text{Co}_{75}\text{Gd}_{25}$ (Fig. 3), in which the net spin precession direction ($\text{Im}[g_t^{\uparrow\downarrow}]$ lagging behind $\text{Re}[g_t^{\uparrow\downarrow}]$) is opposite to that in all other spin sinks ($\text{Im}[g_t^{\uparrow\downarrow}]$ ahead of $\text{Re}[g_t^{\uparrow\downarrow}]$). We speculate that the net magnetization in $\text{Co}_{75}\text{Gd}_{25}$ is slightly dominated by the Gd magnetization, but the direction of the net exchange field – about which the transverse spin current precesses – is governed by the Co

magnetization. Thus, the retrograde spin precession in $\text{Co}_{75}\text{Gd}_{25}$ suggests that transverse spin current interacts somewhat preferentially with the itinerant 3d TM magnetism.

In summary, we have utilized broadband FMR spin pumping to quantify the dephasing length λ_{dp} of transverse spin current in ferrimagnetic CoGd alloys. We obtain a maximum of $\lambda_{dp} \approx 5$ nm in nearly compensated CoGd, consistent with the antiferromagnetic order mitigating the decoherence (dephasing) of transverse spin current. The observed maximum λ_{dp} constitutes a factor of ≈ 4 -5 enhancement compared to that for ferromagnetic metals. Such partial spin rephasing by antiferromagnetic order – even in disordered ferrimagnetic alloys at room temperature – demonstrates a spin-echo-like scheme built into the solid to counter spin decoherence. Our finding also points to the possibility of further extending transverse spin coherence in structurally pristine antiferromagnetic metals, thus opening a new avenue for fundamental studies of spin transport in magnetic media.

Acknowledgements

This research was funded in part by 4-VA, a collaborative partnership for advancing the Commonwealth of Virginia, as well as by the ICTAS Junior Faculty Award and the NSF Grant No. DMR-2003914. We thank Jean J. Heremans for helpful discussions.

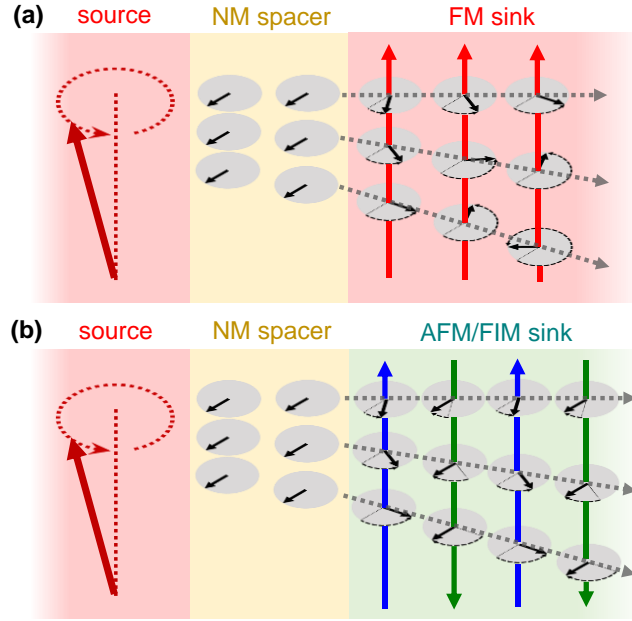


FIG. 1. (Color online) Dephasing of coherent transverse spin current excited by ferromagnetic resonance (FMR) in the spin source. The spin current carried by electrons is coherent in the normal metal (NM) spacer layer (indicated by the aligned black arrows), but enters the spin sink with different incident wavevectors (dashed gray lines). (a) In the FM spin sink, the propagating spins accumulate different precessional phases in the ferromagnetic exchange field (red vertical arrows) and completely dephase within a short distance. (b) In the ideal AFM/FIM, the spin current does not dephase completely in the alternating antiferromagnetic exchange field (blue and green vertical arrows), as any precession at one sublattice is compensated by the opposite precession at the other sublattice.

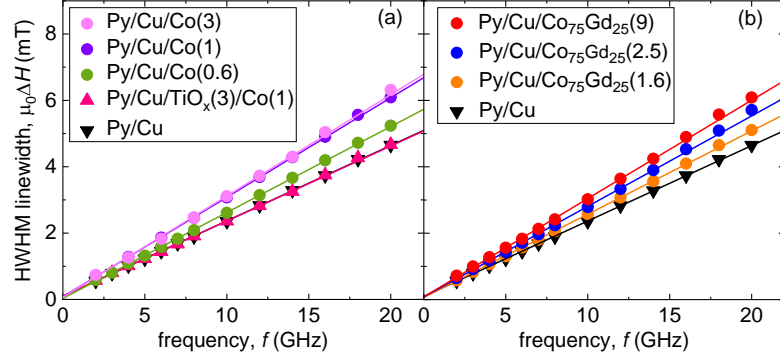


FIG. 2. (Color online) (a) Half-width-at-half-maximum (HWHM) FMR linewidth versus frequency for a stack with a spin sink (NiFe/Cu/Co), stack without a spin sink (NiFe/Cu), and stack with an insulating Ti-oxide spin blocker before the spin sink (NiFe/Cu/TiO_x/Co). (b) FMR linewidth versus frequency for stacks with different Co₇₅Gd₂₅ spin sink thicknesses.

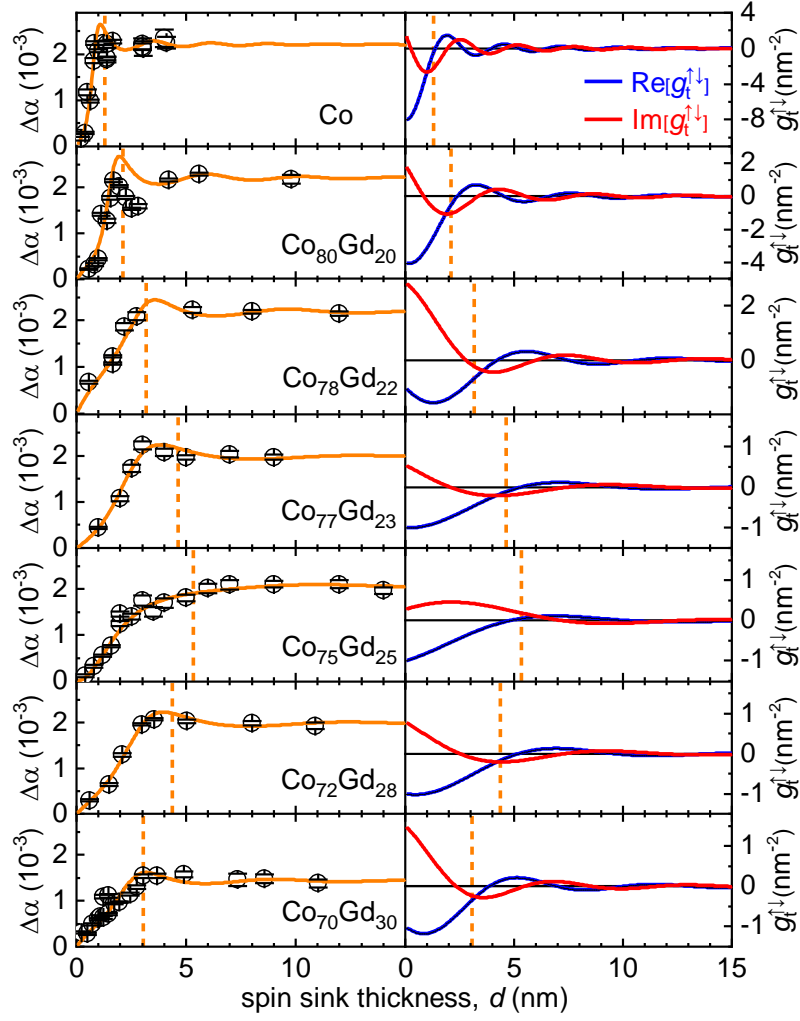


FIG. 3. (Color online) Left column: spin sink thickness dependence of nonlocal damping enhancement $\Delta\alpha$. The solid curve indicates the fit using the modified drift-diffusion model. Right column: spin sink thickness dependence of the real and imaginary parts of the transmitted spin-mixing conductance $g_t^{\uparrow\downarrow}$ derived from the fit. The vertical dashed line indicates the spin dephasing length λ_{dp} .

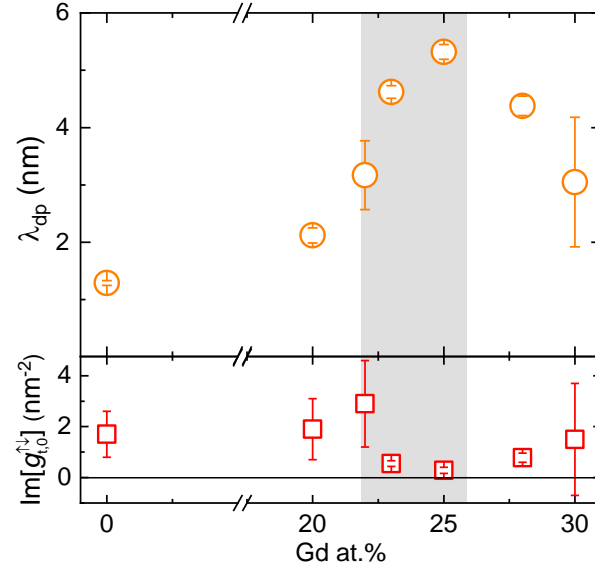


FIG. 4. (Color online) (a) Spin dephasing length λ_{dp} and (b) $\text{Im}[g_t^{\uparrow\downarrow}]$ (related to the net amplitude of spin precession) versus Gd content in the spin sink. The shaded region indicates the window of composition corresponding to magnetic compensation.

1. S. A. Wolf, D. D. Awschalom, R. A. Buhrman, J. M. Daughton, S. von Molnár, M. L. Roukes, A. Y. Chtchelkanova, and D. M. Treger, "Spintronics: a spin-based electronics vision for the future," *Science* (80-.). **294**, 1488–95 (2001).
2. A. Hoffmann and S. D. Bader, "Opportunities at the Frontiers of Spintronics," *Phys. Rev. Appl.* **4**, 47001 (2015).
3. J. Bass and W. P. Pratt, "Spin-diffusion lengths in metals and alloys, and spin-flipping at metal/metal interfaces: an experimentalist's critical review," *J. Phys. Condens. Matter* **19**, 183201 (2007).
4. G. Zahnd, L. Vila, V. T. Pham, M. Cosset-Cheneau, W. Lim, A. Brenac, P. Laczkowski, A. Marty, and J. P. Attané, "Spin diffusion length and polarization of ferromagnetic metals measured by the spin-absorption technique in lateral spin valves," *Phys. Rev. B* **98**, 174414 (2018).
5. M. D. Stiles and A. Zangwill, "Anatomy of spin-transfer torque," *Phys. Rev. B* **66**, 14407 (2002).
6. M. D. Stiles and J. Miltat, "Spin-Transfer Torque and Dynamics," in *Spin Dynamics in Confined Magnetic Structures III* (Springer Berlin Heidelberg, 2006), pp. 225–308.
7. A. Ghosh, S. Auffret, U. Ebels, and W. E. Bailey, "Penetration Depth of Transverse Spin Current in Ultrathin Ferromagnets," *Phys. Rev. Lett.* **109**, 127202 (2012).
8. V. P. Amin and M. D. Stiles, "Spin transport at interfaces with spin-orbit coupling: Phenomenology," *Phys. Rev. B* **94**, 104420 (2016).
9. K.-W. Kim, "Spin transparency for the interface of an ultrathin magnet within the spin dephasing length," *Phys. Rev. B* **99**, 224415 (2019).
10. T. Taniguchi, S. Yakata, H. Imamura, and Y. Ando, "Penetration Depth of Transverse Spin Current in Ferromagnetic Metals," *IEEE Trans. Magn.* **44**, 2636–2639 (2008).
11. A. S. Núñez, R. A. Duine, P. Haney, and A. H. MacDonald, "Theory of spin torques and giant magnetoresistance in antiferromagnetic metals," *Phys. Rev. B* **73**, 214426 (2006).

12. P. M. Haney, D. Waldron, R. A. Duine, A. S. Núñez, H. Guo, and A. H. MacDonald, "Ab initio giant magnetoresistance and current-induced torques in Cr/Au/Cr multilayers," *Phys. Rev. B* **75**, 174428 (2007).
13. Y. Xu, S. Wang, and K. Xia, "Spin-Transfer Torques in Antiferromagnetic Metals from First Principles," *Phys. Rev. Lett.* **100**, 226602 (2008).
14. V. Baltz, A. Manchon, M. Tsoi, T. Moriyama, T. Ono, and Y. Tserkovnyak, "Antiferromagnetic spintronics," *Rev. Mod. Phys.* **90**, 15005 (2018).
15. J. Yu, D. Bang, R. Mishra, R. Ramaswamy, J. H. Oh, H.-J. Park, Y. Jeong, P. Van Thach, D.-K. Lee, G. Go, S.-W. Lee, Y. Wang, S. Shi, X. Qiu, H. Awano, K.-J. Lee, and H. Yang, "Long spin coherence length and bulk-like spin–orbit torque in ferrimagnetic multilayers," *Nat. Mater.* **18**, 29–34 (2019).
16. E. L. Hahn, "Spin Echoes," *Phys. Rev.* **80**, 580–594 (1950).
17. G. S. Uhrig, "Keeping a Quantum Bit Alive by Optimized π -Pulse Sequences," *Phys. Rev. Lett.* **98**, 100504 (2007).
18. F. K. Malinowski, F. Martins, P. D. Nissen, E. Barnes, Ł. Cywiński, M. S. Rudner, S. Fallahi, G. C. Gardner, M. J. Manfra, C. M. Marcus, and F. Kuemmeth, "Notch filtering the nuclear environment of a spin qubit," *Nat. Nanotechnol.* **12**, 16–20 (2016).
19. J. T. Merrill and K. R. Brown, "Progress in Compensating Pulse Sequences for Quantum Computation," in *Quantum Information and Computation for Chemistry* (John Wiley & Sons, Ltd, 2014), pp. 241–294.
20. H. B. M. Saidaoui, A. Manchon, and X. Waintal, "Spin transfer torque in antiferromagnetic spin valves: From clean to disordered regimes," *Phys. Rev. B* **89**, 174430 (2014).
21. A. Manchon, "Spin diffusion and torques in disordered antiferromagnets," *J. Phys. Condens. Matter* **29**, 104002 (2017).
22. A. Ross, R. Lebrun, O. Gomonay, D. A. Grave, A. Kay, L. Baldrati, S. Becker, A. Qaiumzadeh, C. Ulloa, G. Jakob, F. Kronast, J. Sinova, R. Duine, A. Brataas, A.

- Rothschild, and M. Kläui, "Propagation length of antiferromagnetic magnons governed by domain configurations," *Nano Lett.* **acs.nanolett.9b03837** (2019).
23. R. Acharyya, H. Y. T. Nguyen, W. P. Pratt, and J. Bass, "Spin-Flipping Associated With the Antiferromagnet IrMn," *IEEE Trans. Magn.* **46**, 1454–1456 (2010).
 24. P. Merodio, A. Ghosh, C. Lemonias, E. Gautier, U. Ebels, M. Chshiev, H. Béa, V. Baltz, and W. E. Bailey, "Penetration depth and absorption mechanisms of spin currents in Ir 20 Mn 80 and Fe 50 Mn 50 polycrystalline films by ferromagnetic resonance and spin pumping," *Appl. Phys. Lett.* **104**, 32406 (2014).
 25. W. Zhang, M. B. Jungfleisch, W. Jiang, J. E. Pearson, A. Hoffmann, F. Freimuth, and Y. Mokrousov, "Spin Hall effects in metallic antiferromagnets.," *Phys. Rev. Lett.* **113**, 196602 (2014).
 26. B. Khodadadi, Y. Lim, D. A. Smith, R. W. Greening, Y. Zheng, Z. Diao, C. Kaiser, and S. Emori, "Spin decoherence independent of antiferromagnetic order in IrMn," *Phys. Rev. B* **99**, 24435 (2019).
 27. A. Azevedo, L. H. Vilela Leão, R. L. Rodriguez-Suarez, A. B. Oliveira, and S. M. Rezende, "dc effect in ferromagnetic resonance: Evidence of the spin-pumping effect?," *J. Appl. Phys.* **97**, 10C715 (2005).
 28. E. Saitoh, M. Ueda, H. Miyajima, and G. Tatara, "Conversion of spin current into charge current at room temperature: Inverse spin-Hall effect," *Appl. Phys. Lett.* **88**, 182509 (2006).
 29. W. Bailey, P. Kabos, F. Mancoff, and S. Russek, "Control of magnetization dynamics in Ni/sub 81/Fe/sub 19/ thin films through the use of rare-earth dopants," *IEEE Trans. Magn.* **37**, 1749–1754 (2001).
 30. G. Woltersdorf, M. Kiessling, G. Meyer, J.-U. Thiele, and C. H. Back, "Damping by Slow Relaxing Rare Earth Impurities in Ni 80 Fe 20," *Phys. Rev. Lett.* **102**, 257602 (2009).
 31. W. Li, J. Yan, M. Tang, S. Lou, Z. Zhang, X. L. Zhang, and Q. Y. Jin, "Composition and

- temperature-dependent magnetization dynamics in ferrimagnetic TbFeCo," *Phys. Rev. B* **97**, 184432 (2018).
32. P. Hansen, C. Clausen, G. Much, M. Rosenkranz, and K. Witter, "Magnetic and magneto-optical properties of rare-earth transition-metal alloys containing Gd, Tb, Fe, Co," *J. Appl. Phys.* **66**, 756–767 (1989).
 33. M. . Soltani, N. Chakri, and M. Lahoubi, "Composition and annealing dependence of magnetic properties in amorphous Tb–Co based alloys," *J. Alloys Compd.* **323–324**, 422–426 (2001).
 34. B. Hebler, A. Hassdenteufel, P. Reinhardt, H. Karl, and M. Albrecht, "Ferrimagnetic Tb–Fe Alloy Thin Films: Composition and Thickness Dependence of Magnetic Properties and All-Optical Switching," *Front. Mater.* **3**, 8 (2016).
 35. J. P. Andrés, J. L. Sacedón, J. Colino, and J. M. Riveiro, "Interdiffusion up to the eutectic composition and vitrification in Gd/Co multilayers," *J. Appl. Phys.* **87**, 2483 (2000).
 36. T. Taniguchi, S. Yakata, H. Imamura, and Y. Ando, "Determination of Penetration Depth of Transverse Spin Current in Ferromagnetic Metals by Spin Pumping," *Appl. Phys. Express* **1**, 31302 (2008).
 37. X. Qiu, W. Legrand, P. He, Y. Wu, J. Yu, R. Ramaswamy, A. Manchon, and H. Yang, "Enhanced Spin-Orbit Torque via Modulation of Spin Current Absorption," *Phys. Rev. Lett.* **117**, 217206 (2016).
 38. "No Title," in *See Supplemental Material at [Http://link.aps.org/supplemental/xx.xxxx](http://link.aps.org/supplemental/xx.xxxx)* (n.d.).
 39. Y. Tserkovnyak, A. Brataas, and G. Bauer, "Spin pumping and magnetization dynamics in metallic multilayers," *Phys. Rev. B* **66**, 224403 (2002).
 40. J. Li, L. R. Shelford, P. Shafer, A. Tan, J. X. Deng, P. S. Keatley, C. Hwang, E. Arenholz, G. van der Laan, R. J. Hicken, and Z. Q. Qiu, "Direct Detection of Pure ac Spin Current by X-Ray Pump-Probe Measurements," *Phys. Rev. Lett.* **117**, 76602 (2016).
 41. T. Moriyama, M. Kamiya, K. Oda, K. Tanaka, K.-J. Kim, and T. Ono, "Magnetic Moment

- Orientation-Dependent Spin Dissipation in Antiferromagnets," *Phys. Rev. Lett.* **119**, 267204 (2017).
42. T. Mewes, R. L. Stamps, H. Lee, E. Edwards, M. Bradford, C. K. A. Mewes, Z. Tadisina, and S. Gupta, "Unidirectional Magnetization Relaxation in Exchange-Biased Films," *IEEE Magn. Lett.* **1**, 3500204–3500204 (2010).
 43. L. Zhu, D. C. Ralph, and R. A. Buhrman, "Effective Spin-Mixing Conductance of Heavy-Metal–Ferromagnet Interfaces," *Phys. Rev. Lett.* **123**, 57203 (2019).
 44. M. Binder, A. Weber, O. Mosendz, G. Woltersdorf, M. Izquierdo, I. Neudecker, J. R. Dahn, T. D. Hatchard, J.-U. Thiele, C. H. Back, and M. R. Scheinfein, "Magnetization dynamics of the ferrimagnet CoGd near the compensation of magnetization and angular momentum," *Phys. Rev. B* **74**, 134404 (2006).
 45. W. Zhou, T. Seki, T. Kubota, G. E. W. Bauer, and K. Takanashi, "Spin-Hall and anisotropic magnetoresistance in ferrimagnetic Co-Gd/Pt layers," *Phys. Rev. Mater.* **2**, 94404 (2018).
 46. M. A. W. Schoen, J. Lucassen, H. T. Nembach, T. J. Silva, B. Koopmans, C. H. Back, and J. M. Shaw, "Magnetic properties of ultrathin 3d transition-metal binary alloys. I. Spin and orbital moments, anisotropy, and confirmation of Slater-Pauling behavior," *Phys. Rev. B* **95**, 134410 (2017).
 47. J. Finley and L. Liu, "Spin-Orbit-Torque Efficiency in Compensated Ferrimagnetic Cobalt-Terbium Alloys," *Phys. Rev. Appl.* **6**, 54001 (2016).
 48. R. Mishra, J. Yu, X. Qiu, M. Motapothula, T. Venkatesan, and H. Yang, "Anomalous Current-Induced Spin Torques in Ferrimagnets near Compensation," *Phys. Rev. Lett.* **118**, 167201 (2017).
 49. K. Ueda, M. Mann, P. W. P. de Brouwer, D. Bono, and G. S. D. Beach, "Temperature dependence of spin-orbit torques across the magnetic compensation point in a ferrimagnetic TbCo alloy film," *Phys. Rev. B* **96**, 64410 (2017).

50. N. Roschewsky, C.-H. Lambert, and S. Salahuddin, "Spin-orbit torque switching of ultralarge-thickness ferrimagnetic GdFeCo," *Phys. Rev. B* **96**, 64406 (2017).
51. K.-J. Kim, S. K. Kim, Y. Hirata, S.-H. Oh, T. Tono, D.-H. Kim, T. Okuno, W. S. Ham, S. Kim, G. Go, Y. Tserkovnyak, A. Tsukamoto, T. Moriyama, K.-J. Lee, and T. Ono, "Fast domain wall motion in the vicinity of the angular momentum compensation temperature of ferrimagnets," *Nat. Mater.* **16**, 1187–1192 (2017).
52. S.-G. Je, J.-C. Rojas-Sánchez, T. H. Pham, P. Vallobra, G. Malinowski, D. Lacour, T. Fache, M.-C. Cyrille, D.-Y. Kim, S.-B. Choe, M. Belmeguenai, M. Hehn, S. Mangin, G. Gaudin, and O. Boulle, "Spin-orbit torque-induced switching in ferrimagnetic alloys: Experiments and modeling," *Appl. Phys. Lett.* **112**, 62401 (2018).
53. L. Caretta, M. Mann, F. Büttner, K. Ueda, B. Pfau, C. M. Günther, P. Helsing, A. Churikova, C. Klose, M. Schneider, D. Engel, C. Marcus, D. Bono, K. Bagschik, S. Eisebitt, and G. S. D. Beach, "Fast current-driven domain walls and small skyrmions in a compensated ferrimagnet," *Nat. Nanotechnol.* **1** (2018).
54. S. Woo, K. M. Song, X. Zhang, Y. Zhou, M. Ezawa, X. Liu, S. Finizio, J. Raabe, N. J. Lee, S.-I. Kim, S.-Y. Park, Y. Kim, J.-Y. Kim, D. Lee, O. Lee, J. W. Choi, B.-C. Min, H. C. Koo, and J. Chang, "Current-driven dynamics and inhibition of the skyrmion Hall effect of ferrimagnetic skyrmions in GdFeCo films," *Nat. Commun.* **9**, 959 (2018).
55. R. Bläsing, T. Ma, S.-H. Yang, C. Garg, F. K. Dejene, A. T. N'Diaye, G. Chen, K. Liu, and S. S. P. Parkin, "Exchange coupling torque in ferrimagnetic Co/Gd bilayer maximized near angular momentum compensation temperature," *Nat. Commun.* **9**, 4984 (2018).
56. Y. Hirata, D.-H. Kim, S. K. Kim, D.-K. Lee, S.-H. Oh, D.-Y. Kim, T. Nishimura, T. Okuno, Y. Futakawa, H. Yoshikawa, A. Tsukamoto, Y. Tserkovnyak, Y. Shiota, T. Moriyama, S.-B. Choe, K.-J. Lee, and T. Ono, "Vanishing skyrmion Hall effect at the angular momentum compensation temperature of a ferrimagnet," *Nat. Nanotechnol.* **14**, 232–236 (2019).

57. C. Kaiser, A. F. Panchula, and S. S. P. Parkin, "Finite Tunneling Spin Polarization at the Compensation Point of Rare-Earth-Metal–Transition-Metal Alloys," *Phys. Rev. Lett.* **95**, 47202 (2005).
58. X. Jiang, L. Gao, J. Z. Sun, and S. S. P. Parkin, "Temperature Dependence of Current-Induced Magnetization Switching in Spin Valves with a Ferrimagnetic CoGd Free Layer," *Phys. Rev. Lett.* **97**, 217202 (2006).
59. B. Heinrich, "Spin Relaxation in Magnetic Metallic Layers and Multilayers," in *Ultrathin Magnetic Structures III*, J. A. C. Bland and B. Heinrich, eds. (Springer-Verlag, 2005), pp. 143–210.
60. S. S. Kalarickal, P. Krivosik, M. Wu, C. E. Patton, M. L. Schneider, P. Kabos, T. J. Silva, and J. P. Nibarger, "Ferromagnetic resonance linewidth in metallic thin films: Comparison of measurement methods," *J. Appl. Phys.* **99**, 93909 (2006).
61. M. A. W. Schoen, J. Lucassen, H. T. Nembach, T. J. Silva, B. Koopmans, C. H. Back, and J. M. Shaw, "Magnetic properties in ultrathin 3d transition-metal binary alloys. II. Experimental verification of quantitative theories of damping and spin pumping," *Phys. Rev. B* **95**, 134411 (2017).
62. C. H. Du, H. L. Wang, Y. Pu, T. L. Meyer, P. M. Woodward, F. Y. Yang, and P. C. Hammel, "Probing the spin pumping mechanism: exchange coupling with exponential decay in Y3Fe5O12/barrier/Pt heterostructures.," *Phys. Rev. Lett.* **111**, 247202 (2013).
63. A. A. Baker, A. I. Figueroa, D. Pingstone, V. K. Lazarov, G. van der Laan, and T. Hesjedal, "Spin pumping in magnetic trilayer structures with an MgO barrier," *Sci. Rep.* **6**, 35582 (2016).
64. A. Azevedo, L. H. Vilela-Leão, R. L. Rodríguez-Suárez, A. F. Lacerda Santos, and S. M. Rezende, "Spin pumping and anisotropic magnetoresistance voltages in magnetic bilayers: Theory and experiment," *Phys. Rev. B* **83**, 144402 (2011).
65. L. Bai, P. Hyde, Y. S. Gui, C.-M. Hu, V. Vlainck, J. E. Pearson, S. D. Bader, and A.

- Hoffmann, "Universal Method for Separating Spin Pumping from Spin Rectification Voltage of Ferromagnetic Resonance," *Phys. Rev. Lett.* **111**, 217602 (2013).
66. M. Obstbaum, M. Härtinger, H. G. Bauer, T. Meier, F. Swientek, C. H. Back, and G. Woltersdorf, "Inverse spin Hall effect in Ni₈₁Fe₁₉/normal-metal bilayers," *Phys. Rev. B* **89**, 60407 (2014).
 67. H. Schultheiss, J. E. Pearson, S. D. Bader, and A. Hoffmann, "Thermoelectric Detection of Spin Waves," *Phys. Rev. Lett.* **109**, 237204 (2012).
 68. K. Yamanoi, M. Yafuso, K. Miyazaki, and T. Kimura, "Signature of spin-dependent Seebeck effect in dynamical spin injection of metallic bilayer structures," *J. Phys. Mater.* **3**, 14005 (2019).
 69. C. T. Boone, H. T. Nembach, J. M. Shaw, and T. J. Silva, "Spin transport parameters in metallic multilayers determined by ferromagnetic resonance measurements of spin-pumping," *J. Appl. Phys.* **113**, 153906 (2013).
 70. E. Montoya, P. Omelchenko, C. Coutts, N. R. Lee-Hone, R. Hübner, D. Broun, B. Heinrich, and E. Girt, "Spin transport in tantalum studied using magnetic single and double layers," *Phys. Rev. B* **94**, 54416 (2016).
 71. A. A. Baker, A. I. Figueroa, C. J. Love, S. A. Cavill, T. Hesjedal, and G. van der Laan, "Anisotropic Absorption of Pure Spin Currents," *Phys. Rev. Lett.* **116**, 47201 (2016).
 72. M. Caminale, A. Ghosh, S. Auffret, U. Ebels, K. Ollefs, F. Wilhelm, A. Rogalev, and W. E. Bailey, "Spin pumping damping and magnetic proximity effect in Pd and Pt spin-sink layers," *Phys. Rev. B* **94**, 14414 (2016).
 73. A. A. Kovalev, G. E. W. Bauer, and A. Brataas, "Perpendicular spin valves with ultrathin ferromagnetic layers: Magnetoelectronic circuit investigation of finite-size effects," *Phys. Rev. B* **73**, 54407 (2006).
 74. M. Zwierzycki, Y. Tserkovnyak, P. J. Kelly, A. Brataas, and G. E. W. Bauer, "First-principles study of magnetization relaxation enhancement and spin transfer in thin

- magnetic films," *Phys. Rev. B* **71**, 64420 (2005).
75. Y. Tserkovnyak, A. Brataas, G. E. W. Bauer, and B. I. Halperin, "Nonlocal magnetization dynamics in ferromagnetic heterostructures," *Rev. Mod. Phys.* **77**, 1375–1421 (2005).
 76. V. G. Harris, K. D. Aylesworth, B. N. Das, W. T. Elam, and N. C. Koon, "Structural origins of magnetic anisotropy in sputtered amorphous Tb-Fe films," *Phys. Rev. Lett.* **69**, 1939–1942 (1992).
 77. P. M. Haney, R. A. Duine, A. S. Núñez, and A. H. MacDonald, "Current-induced torques in magnetic metals: Beyond spin-transfer," *J. Magn. Magn. Mater.* **320**, 1300–1311 (2008).
 78. A. N. Chantis, M. Van Schilfgaarde, and T. Kotani, "Quasiparticle self-consistent GW method applied to localized 4f electron systems," *Phys. Rev. B* **76**, 165126 (2007).
 79. B. Frietsch, J. Bowlan, R. Carley, M. Teichmann, S. Wienholdt, D. Hinzke, U. Nowak, K. Carva, P. M. Oppeneer, and M. Weinelt, "Disparate ultrafast dynamics of itinerant and localized magnetic moments in gadolinium metal," *Nat. Commun.* **6**, 8262 (2015).
 80. Y. Mimura, N. Imamura, and Y. Kushiro, "Hall effect in rare-earth–transition-metal amorphous alloy films," *J. Appl. Phys.* **47**, 3371–3373 (1976).
 81. W. H. Butler, "Tunneling magnetoresistance from a symmetry filtering effect," *Sci. Technol. Adv. Mater.* **9**, 14106 (2008).
 82. S. Zhang, P. M. Levy, and A. Fert, "Mechanisms of Spin-Polarized Current-Driven Magnetization Switching," *Phys. Rev. Lett.* **88**, 236601 (2002).